Supporting Information

The Enhanced Electrocatalytic Performance ofNanoscopic $Cu_6Pd_{12}Fe_{12}$Heterometallic Molecular Box Encaged Cytochrome c

Shazia Nabi[a], Feroz Ahmad Sofi[a], Qounsar Jan[a], Aamir Y. Bhat[b], Pravin P. Ingole[b], Maryam Bayati[c], Mohsin Ahmad Bhat[a,*]

[a,*]*Department of Chemistry, University of Kashmir, Srinagar-190006, J & K, India. E-mail: mohsin@kashmiruniversity.ac.inTel: +91 9419033125*

[b]*Department of Chemistry, Indian Institute of Technology (IIT) Delhi, New Delhi, India 110016.*

[c]*Department of Mechanical & Construction Engineering, Faculty of Engineering and Environment, Northumbria University, Newcastle upon Tyne, NE1 8ST, UK.*

Scheme:

Scheme-S1: Illustration of synthetic scheme employed for the synthesis of Cu-HMHMB using slightly modified reported protocol.

Tables:

Table-S1: ICP-MS Elemental analysis

Table-S2: Estimation of recovery of spiked nitrite in real sample by DPV method over the proposed Cyt-c@Cu-HMHMB/GCE based biosensor.

Table-S3: Peak attributes for oxygen reduction reaction in 0.1M PBS for bare GCE, Cu-HMHMB/GCE and Cyt-c@Cu- HMHMB/GCE

Figures:

Figure-S1: ^{1}H-NMR spectrum of HMHMB, Cu-HMHMB and Cyt-c@Cu-HMHMB

Figure-S2: EDX spectrum of Cyt-c@Cu-HMHMB depicting the distribution of nitrogen (N), copper (Cu), palladium (Pd) and iron (Fe) within the bio-composite.

Figure-S3: TGA curves recorded over Cu-HMHMB **(a)** and Cyt-c@Cu-HMHMB/GCE **(b)** in N_2 atmosphere.

Figure-S4: TEM image of Cu-HMHMB heterometallic cage **(a)**, and Cyt-c loaded Cu-HMHMB Composite **(b)**

Figure-S5: Circular Dichroism (CD) spectra of cytochrome c and Cyt-c@Cu-HMHMB in the far-UV region (250-200 nm) **[panel A]** and near-UV region of wavelength range (350-270 nm) **[panel B].**Dynamic Light Scattering (DLS) Analysis of Cu-HMHMB (a) and Cyt-c@Cu-HMHMB (b) depicting the particle size distribution of the Cu-HMHMB before and after encaging of Cytochrome c **[panel C].**

Figure-S6: Cyclic Voltammogram corresponding to Cytochrome c over bare GCE in 0.1M phosphate buffer solution (pH=7.2) at 50 mV/s.

Figure-S7: CVs recorded over Cu-HMHMB/GCE **[panel A]** and Cyt-c@Cu-HMHMB/GCE **[panel B]** showing variation of I_{pa} and I_{pc} with scan rate (ν) changing from 20mV/s to 200mV/s. Inset showing linear fits of I_p vs. square root of scan rate ($\nu^{1/2}$) in case of Cu-HMHMB/GCE **[panel A]** and I_p vs. scan rate(ν) and E_p vs ln(scan rate) for Cyt-c@Cu-HMHMB/GCE [**panel B].**

Figure-S8: CVs recorded for 2mM $Fc(CH_2OH)$ in 0.1M KNO_3 over Cyt-c @Cu-HMHMB/GCE at changing scan rate ranging from 10mV/s -500mV/s **[panel A]**. Inset showing **v**ariation of I_{pa} and I_{pc} with scan rate ($\nu^{1/2}$) changing from 10mV/s to 500mV/s for Cyt-c@Cu-HMHMB /GCE. Chronocoulometric response for Cu-HMHMB/GCE (black trace) and Cyt-c@Cu-HMHMB/GCE (red trace) in 2mM $Fc(CH_2OH)$ with 0.1M KNO_3 as supporting electrolyte **[panel B]**.

Figure-S9: Square-wave forward and reverse current voltammograms for Cyt-c@Cu-HMHMB/GCE in 0.1M phosphate buffer solution with different pH ranging from 5.0-9.0 SWV condition: pulse height: 75 mV, step height 2 mV, and frequency 180 Hz **[panel A].** Effect of pH on formal redox potential ($E^{0'}$) estimated from SWVs for Cyt-c@Cu-HMHMB composite at a scan rate of 50mV/s **[panel B].**

Figure-S10: CVs recorded for 2mM$NaNO_2$in 0.1M phosphate buffer solution (pH=7.2) over Cyt-c @Cu HMHMB/GCE at changing scan rate ranging from 10mV/s -500 mV/s. Inset showing variation

of I_{pa} with scan rate ($v^{1/2}$) **[panel A]**. CVs recorded over Cyt-c@Cu-HMHMB/GCE at changing concentration of $NaNO_2$in 0.1M phosphate buffer solution (pH=7.2) in the range of 0.5mM-2mM at a constant scan rate of 50mV/s. Inset showing the variation of I_{pa} with the concentration of nitrite ion **[panel B].**

Figure-S11: Experimental limiting current chronoamperogram recorded at post peak potential in the presence of 2mM nitrite ion in 0.1M PBS (pH 7.2) over Cyt-c@Cu-HMHMB/GCE. Dotted line shows the best-fit theoretical curve predicting the electrocatalytic mechanism (EC′) for electro-oxidation of nitrite ion.

Figure-S12: LSVs recorded in O_2 saturated solution of 0.1M PBS (pH=7.2) Cu-HMHMB/GCE **[panel A]** and Cyt-c@Cu-HMHMB **[panel B]** at different disk rotation rates (100 rpm to 2000 rpm) at a scan rate of 50 mV/s.

Figure-S13: EIS studies showing Nyquist plots at varying potentials of oxygen reduction reaction over Cu-HMHMB/GCE **[panel-A]** and Cyt-c@Cu-HMHMB/GCE **[panel-B]**; Chronoamperometric curve at E=0.1V vs. RHE in 0.1M PBS (pH 7.2) over Cyt-c@Cu-HMHMB/GCE for about 30,000 seconds **[panel-C].**

Figure-S14: TEM image recorded for the Cyt-c@Cu-HMHMB nanocomposite pre-Electrolysis **[panel A]** and post-Electrolysis tests **[panel-B]**

S1. EXPERIMENTAL SECTION.

S1.1. Reagents and Materials

All the chemicals and reagents, including 5,10,15,20-Tetrakis(4-pyridyl)-21H,23H-porphine (TPyP)(97%),CF_3SO_3Ag(≥99%),1,1′bis(diphenylphosphino)ferrocenedichloropalladium(II)(98%) ,hexaammineruthenium(III)trichloride (98%) and Copper(II) acetate (98%) ($Cu(OAC)_2$),sodium dihydrogen phosphate, disodium hydrogen phosphate were procured from Merck, disodium hydrogen phosphate were procured from Merck. Cytochrome c (Cyt-c) (Horse Heart extra pure (90%)) was obtained from SRL Pvt. Ltd. N,N- dimethylformamide (DMF, anhy. 99.8%) diethyl ether, ethanol and nitromethane (≥ 95%) were purchased from Merck and dichloromethane from Spectrochem India. All the chemicals and reagents were of analytical grade and were used without

further purification. All the studies were carried out in 0.1M phosphate buffer saline (PBS) of pH 7.2 at 25 ±0.1^{o}C.All the experiments were performed using ultrapure Triple distilled water.

S1.2. Instrumentation

The nanocomposites were characterized through various spectroscopic and microscopic techniques including UV-Vis absorption spectroscopy with diffused reflectance spectroscopy (DRS) attachment, FTIR, ^{1}H-NMR spectroscopy and Inductively Coupled plasma mass spectrometry (ICP-MS). The UV-Vis measurements were carried on solid samples using Perkin Elmer UV-Vis/NIR lambda-750 spectrophotometer equipped with an integrating sphere attachment. $BaSO_4$ standard was used as the reference. The Fourier transform infrared (FTIR) spectra of the samples were recorded on Perkin Elmer ATR-FTIR spectrometer. The ^{1}H-NMR-500MHz spectra were recorded at room temperature using deuterated solvents as internal standard on a FT-NMR model Avance Neo (Bruker) spectrometer. Electrochemical measurements were performed on Metrohm Autolab potentiostat/galvanostat (PGSTAT-100N) in a three-electrode set-up with glassy carbon (GCE, 2 mm diameter) or GCE modified with Cu-HMHMB and Cyt-c@Cu-HMHMB as working electrode (WE), platinum wire as counter electrode (CE) and Ag/AgCl, 3M KCl as reference electrode (RE). Scanning electron microscopy (SEM) images were obtained from Zeiss EVO50: ZEISS, Germany. The transmission electron microscopy (TEM) imaging was carried using a JEOL JEM 1400 microscope (Japan Electron Optics Laboratory Co., Ltd, Japan) working at an accelerating voltage of 120 kV. ICP-MS measurements were performed on Agilent ICP-MS 7900 with UHMI.TGA analysis was carried on Simultaneous Thermal Analyzer SDT650 with N_2 gas flow as an inert atmosphere. The Circular Dichroism spectra were recorded using MOS-500 spectropolarimeter (Bio Logic, France) with a 0.1 cm path length over the 190-400 nm range. The samples were prepared in 0.1M phosphate buffer (pH 7.0). Each spectrum was obtained as an

average of three scans to reduce noise and smoothed before structure analysis was made. The particle size distribution of the samples was recorded using Dynamic light scattering. The data was collected on Particle Analyzer (DLS), Anton Paar (Litesizer-500) operating at 25°C.

S1.3. Preparation of Cu-HMHMB and Cyt-c@Cu-HMHMB composite

Following a previously published process with a minor modification [S1], nanoscopic $Cu_6Pd_{12}Fe_{12}$ heterometallic hexagonal molecular boxes (Cu-HMHMB) were crafted according to **Scheme-S1**.We approached the synthesis by replacing 5,10, 15, 20-Tetrakis(4-pyridyl)-21H, 23H-porphine (TPyP) by M(TPyP), where M = Cu^{2+}. The synthesis of Cu(TPyP) was achieved by following the procedure as follows: H_2TPyP was added to a $Cu(OAc)_2.H_2O$ (0.02g) solution in a CH_3OH and DMF mixture and the reaction was stirred at room temperature (25 ºC). Centrifugation was used to separate the precipitate once it had been produced, which was then washed many times before being dried at room temperature. To proceed further, a solution of cis-[(dppf)Pd$(OTf)_2$] (21.0 mg, 0.02 mmol) in nitromethane (4 mL) was added drop wise to the solution of Cu[TPyP] (10.4 mg, 0.01 mmol) in dichloromethane (2 mL) in a 10 mL round-bottom flask with continuous stirring for 15 min. A distinct colour change from purple to red-brown was observed, and the mixture was further stirred for 2.5 h at 80 ºC. Diethyl ether was added to the reaction mixture after it had cooled to room temperature to separate the Cu-HMHMB as a reddish-brown precipitate.

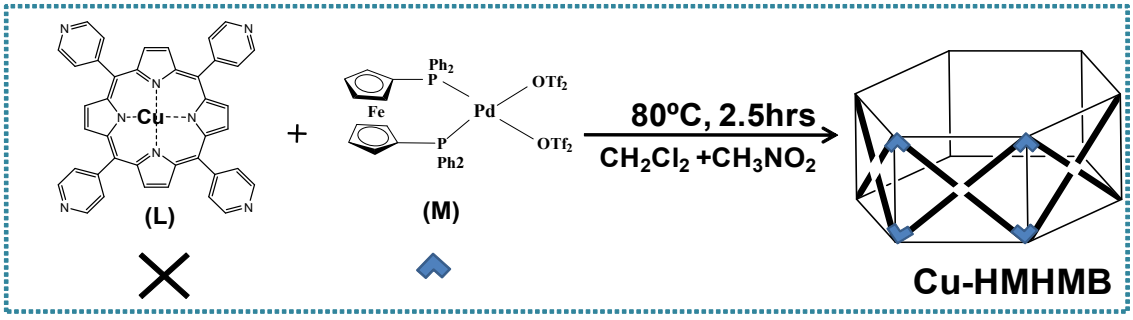

Scheme-S1. *Illustration of synthetic scheme employed for the synthesis of Cu-HMHMB using slightly modified reported protocol [S1].*

The as-synthesized Cu-HMHMB is a barrel with six tetratopic Cu[TPyP] units occupying the faces, and Pd(II) acceptors occupying the vertices. The framework is reported to be very rigid with an inner cavity quite large with dimensions of 27×27×19 $Å^3$, with an internal void volume estimated to be approximately 43550$Å^3$ [S1].These physicochemical, structural, and geometrical characteristics of the as-synthesized Cu-HMHMB point to its suitability for Cyt-c (3.2nm × 2.7nm × 3.3nm) entrapment *via* its special host-guest chemistry.For the synthesis of Cyt-c@Cu-HMHMB composite, 5mg of the Cu-HMHMB crystals were soaked in 5 mL aqueous solution of cytochrome c in 0.1 M phosphate buffer (pH=7.2). The suspension was kept under mild stirring at room temperature for 48hrs to ensure the effective encapsulation of Cyt-c within the Cu-HMHMB. The suspension was centrifuged to produce the Cyt-c@Cu-HMHMB composite, which was then washed in water and allowed to dry at room temperature.

S1.4. Electrode Preparation for Electrochemical Investigations

Prior to electrode fabrication, catalyst inks of Cyt-c@Cu-HMHMB composite and Cu-HMHMB were prepared by dispersing 1mg of the sample in 1 mL water by sonication for 20 min in an ultra-sonicator bath. The glassy carbon electrode (GCE) was thoroughly rinsed with acetone, ethanol, and triple-distilled water after being polished with alumina slurry to get a mirror-like electrode surface. 10 µL of catalyst ink was drop-casted over the clean GCE surface for the preparation of electrocatalyst-modified GCE for electrochemical studies.

S1.5. Electrochemical Measurements

All the electrochemical tests were performed with Metrohm Autolab potentiostat/galvanostat workstation (PGSTAT-100) in a three-electrode set-up with glassy carbon or GCE modified with

Cu-HMHMB and Cyt-c@Cu-HMHMB as WE, platinum wire as CE and Ag/AgCl, 3M KCl as RE. Prior to using for electrochemical measurements, these were properly cleaned, washed several times with Millipore water and wiped off with soft tissue soaked in ethanol. The experiments related to ORR tests are performed in 0.1M phosphate buffer solution of pH=7.2 and all the potential values reported for ORR are normalized to reversible hydrogen electrode (RHE) based on the equation:

$$E(RHE) = E(Ag/AgCl) + 0.0591pH + E^0(Ag/AgCl) \quad (S1)$$

where, $E^0(Ag/AgCl) = 0.1976$ V at 25 ^{0}C.

Table.S1:*ICP-MS Elemental Analysis*

Electrocatalyst	Cu(mg)	Fe(mg)
Cu-HMHMB	0.1439	0.0262
Cyt-c@Cu-HMHMB	0.2046	0.0448

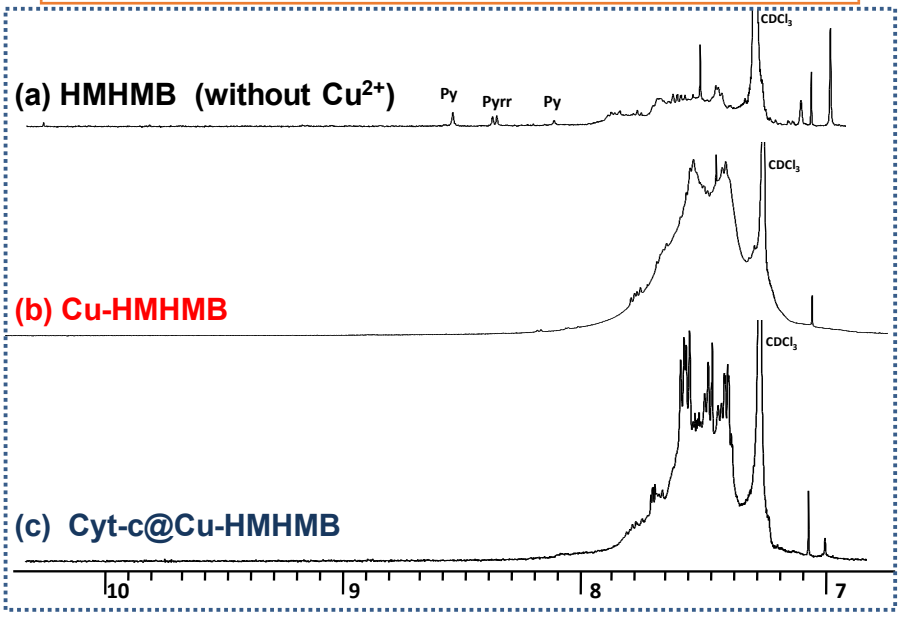

Figure-S1: *^{1}H-NMR spectrum of HMHMB **(a)**, Cu-HMHMB **(b)**, and Cyt-c@Cu-HMHMB**(c)***

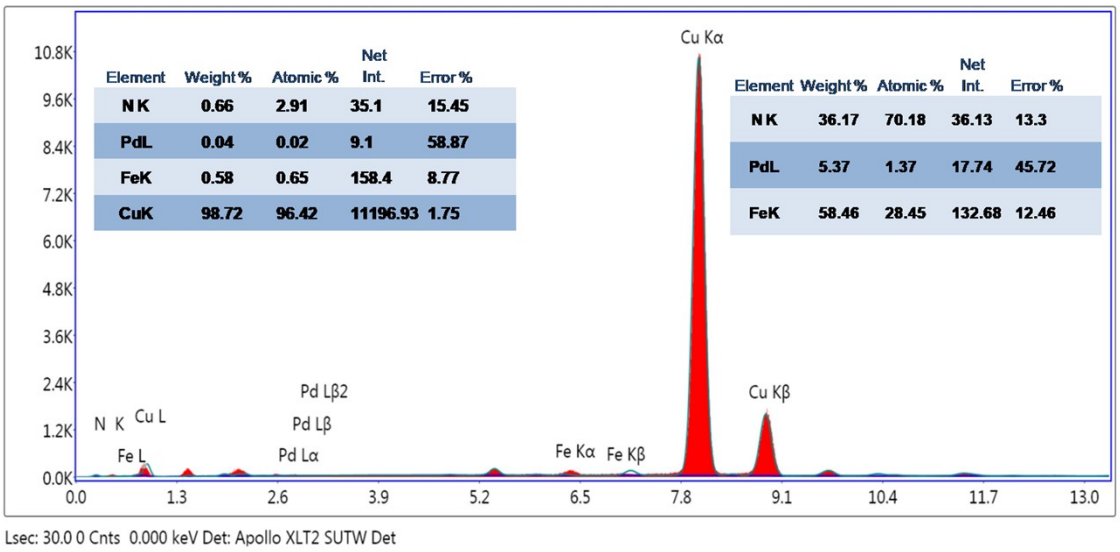

Figure-S2: *EDX spectrum of Cyt-c@Cu-HMHMB depicting the distribution of nitrogen (N), copper (Cu), palladium (Pd) and iron (Fe) within the bio-composite.*

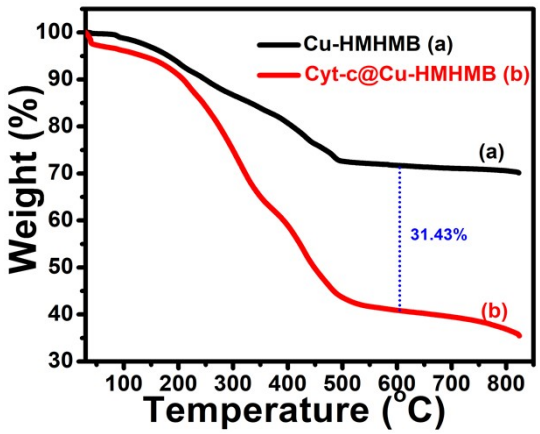

Figure-S3: *TGA curves recorded over Cu-HMHMB* ***(a)*** *and Cyt-c@Cu-HMHMB* ***(b)***

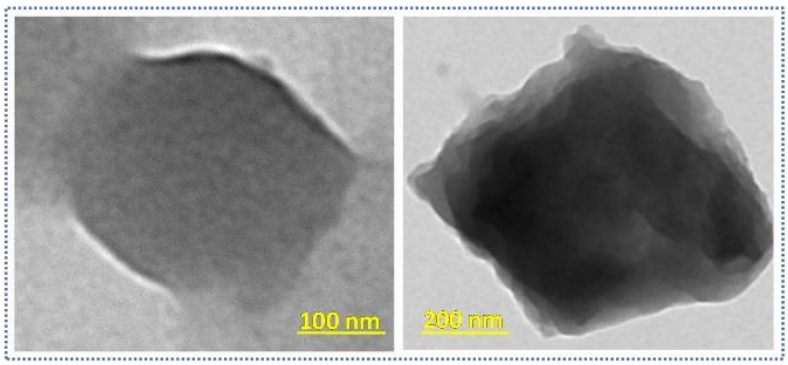

Figure-S4: *TEM image of Cu-HMHMB heterometallic cage* ***(a)****, and Cyt-c loaded Cu-HMHMB composite* ***(b)***

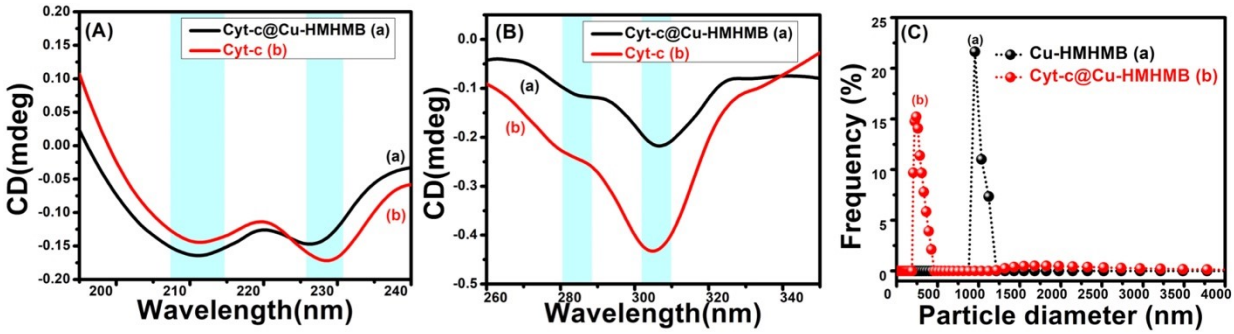

Figure-S5: *Circular Dichroism (CD) spectra of cytochrome c and Cyt-c@Cu-HMHMB in the far-UV region (250–200 nm)* ***[panel A]*** *and near-UV region of wavelength range 350–270 nm* ***[panel B];*** *Dynamic Light Scattering (DLS) Analysis of Cu-HMHMB* ***(a)*** *and Cyt-c@Cu-HMHMB* ***(b)*** *depicting the particle size distribution of the Cu-HMHMB before and after encaging of Cytochrome c* ***[panel C].***

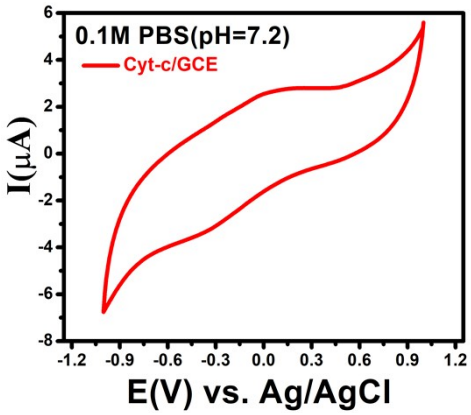

Figure-S6: *Cyclic Voltammogram corresponding to Cytochrome c over bare GCE in 0.1 M phosphate buffer solution (pH=7.2) at 50mV/s.*

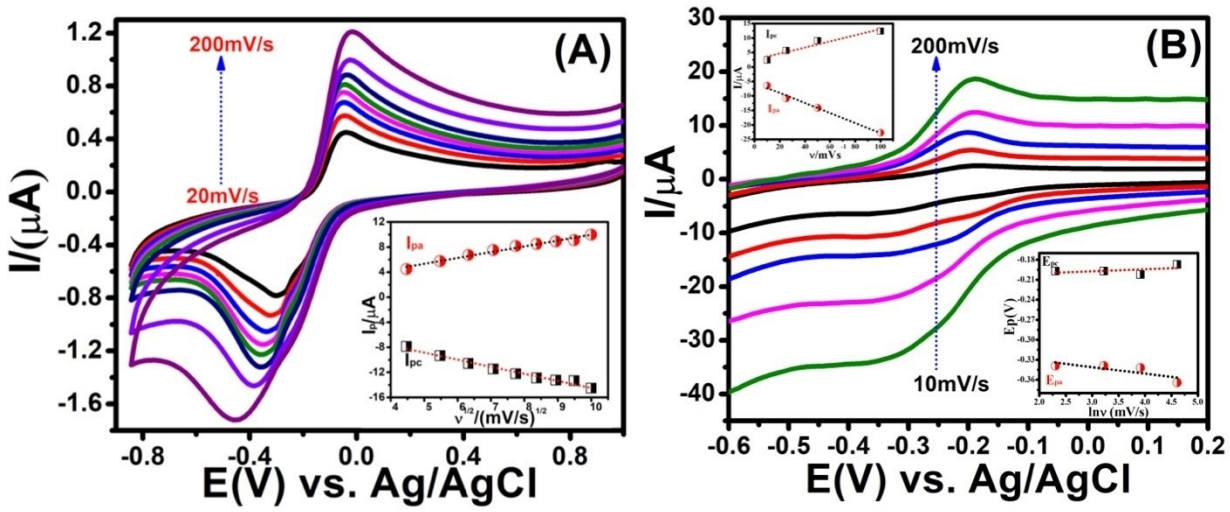

Figure-S7: *CVs recorded over Cu-HMHMB/GCE* ***[panel A]*** *and Cyt-c@Cu-HMHMB/GCE* ***[panel B]*** *showing variation of I_{pa} and I_{pc} with scan rate (v) changing from 20mV/s to 200mV/s. Inset showing linear fits of I_p vs.square root of scan rate ($v^{1/2}$) in case of Cu-HMHMB/GCE* ***[panel A]*** *and Ip vs. scan rate(v) and E_p vs. ln(scan rate) for Cyt-c@Cu-HMHMB/GCE [****panel B].***

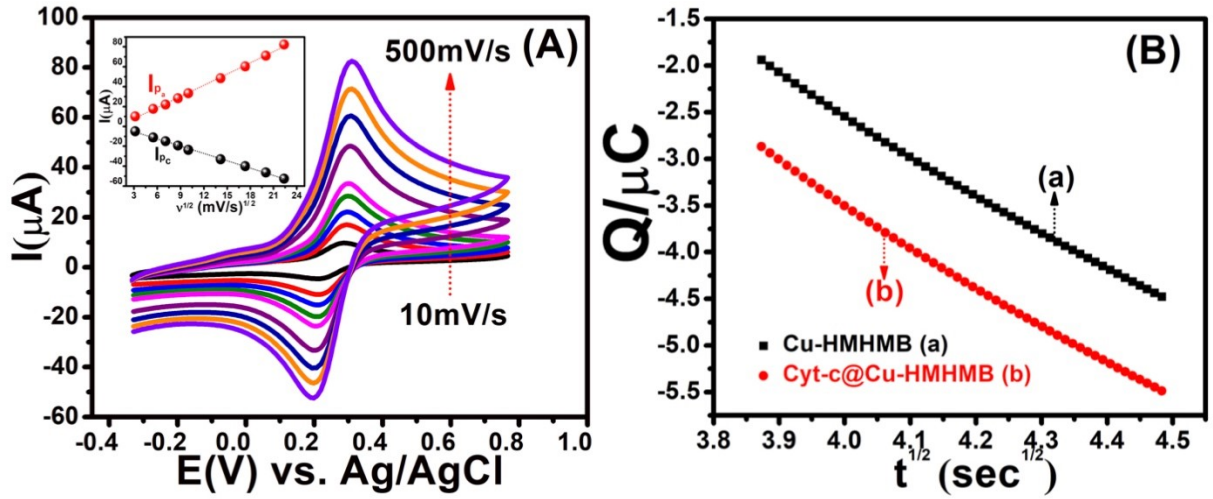

Figure-S8: *CVs recorded for 2mM $Fc(CH_2OH)$ in 0.1M KNO_3 over Cyt-c @Cu-HMHMB/GCE at changing scan rate ranging from 10mV/s -500mV/s* ***[panel A]****. Inset showing* ***v****ariation of I_{pa} and I_{pc} with scan rate ($v^{1/2}$) changing from 10mV/s to 500mV/s for Cyt-c @Cu-HMHMB /GCE. Chronocoulometric response for Cu-HMHMB/GCE (black trace) and Cyt-c @Cu-HMHMB/GCE (red trace) in 2mM $Fc(CH_2OH)$ with 0.1M KNO_3 as supporting electrolyte* ***[panel B]****.*

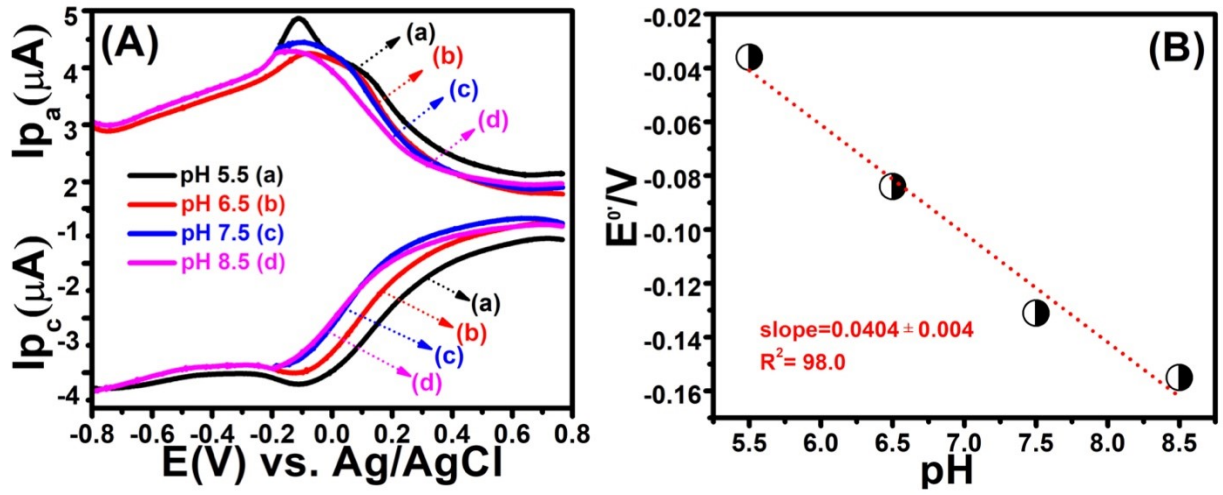

Figure-S9: *Square wave forward and reverse current voltammograms for Cyt-c@Cu-HMHMB/GCE in 0.1M phosphate buffer solution with different pH ranging from 5.0-9.0. SWV condition: pulse height: 75 mV, step height 2 mV, and frequency 180 Hz* ***[panel A].*** *Effect of pH on formal redox potential ($E^{0'}$) estimated from SWVs for Cyt-c@Cu-HMHMB composite at a scan rate of 50mV/s* ***[panel B].***

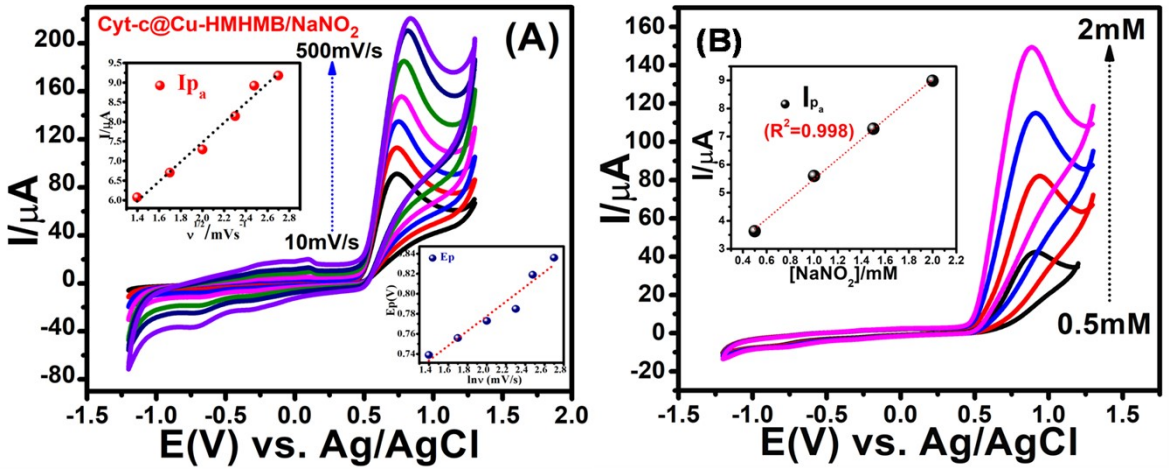

Figure-S10:*CVs recorded for 2mM$NaNO_2$in 0.1M phosphate buffer solution (pH=7.2) overCyt-c @Cu HMHMB/GCEat changing scan rate ranging from 10mV/s -500mV/s. Insetshowing variation of I_{pa} with scan rate ($v^{1/2}$)* ***[panel A]****. CVs recorded overCyt-c @Cu-HMHMB/GCE at changing concentration of $NaNO_2$in 0.1M phosphate buffer solution (pH=7.2) in the range of 0.5mM-2mM at a constant scan rate of50mV/s. Insetshowing the variation of I_{pa} with the concentration of nitrite ion* ***[panel B]****.*

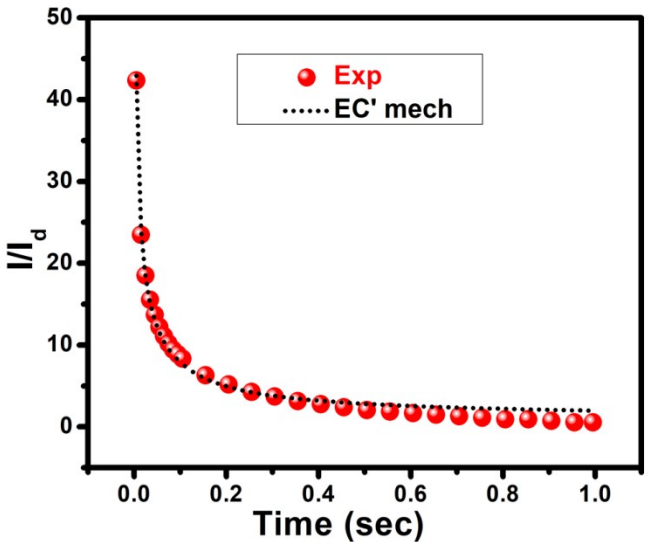

Figure-S11: *Experimental limiting current chronoamperogram recorded at post peak potential in the presence of 2mM nitrite ion in 0.1M PBS (pH 7.2) over Cyt-c@Cu-HMHMB/GCE. Dotted line shows the best-fit theoretical curve predicting the electrocatalytic mechanism (EC') for electro-oxidation of nitrite ion.*

Table.S2: *Estimation of recovery of spiked nitrite in real sample by DPV method over the proposed Cyt-c@Cu-HMHMB/GCE based biosensor.*

Sample	Spiked $[NO_2^-]$/(μM)	Amount Recovered	Recovery (%)	RSD (%)
Tap water	30	29.90	99.80	1.00
	40	39.42	98.55	1.10
	50	49.30	98.66	1.02

Table.S3:*Peak attributes for oxygen reduction reaction in 0.1M PBS (pH=7.2) for bare GCE, Cu-HMHMB/GCE and Cyt-c@Cu- HMHMB/GCE.*

Catalyst	E_{onset} (V vs. RHE)	$E_{half\ wave}$ (V vs. RHE)	O_2 reduction wave potential (V vs. RHE)
Bare GCE	0.041	-0.110	-0.369

Cu-HMHMB	0.173	0.024	-0.278
Cyt-c@Cu-HMHMB	0.322	0.078	-0.108

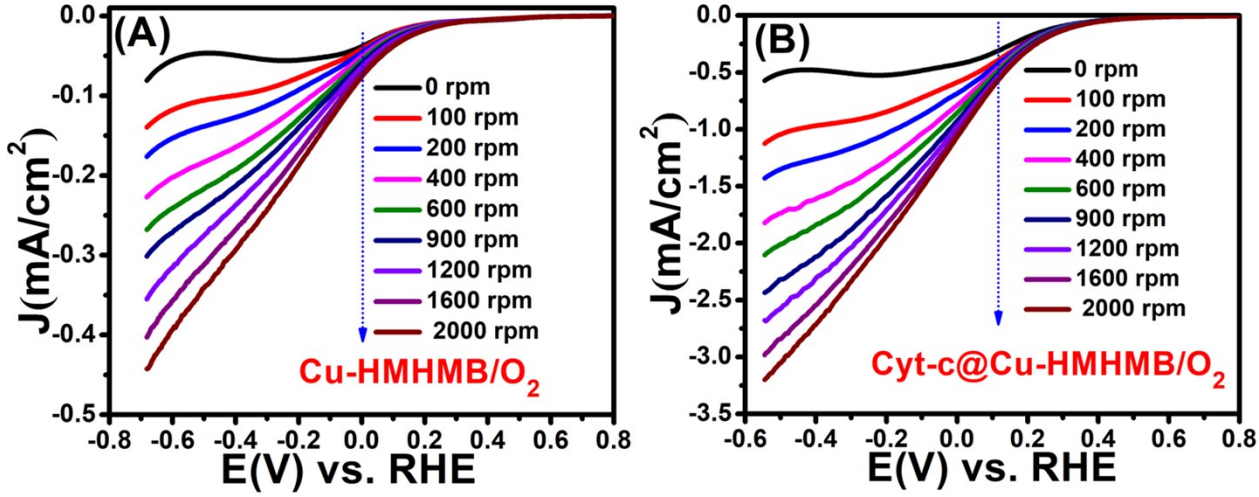

Figure-S12:*LSVs recorded in O_2 saturated solution of 0.1M PBS (pH=7.2) Cu-HMHMB/GCE* ***[panel A]*** *and Cyt-c@Cu-HMHMB* ***[panel B]*** *at different disk rotation rates(100rpm to 2000rpm)at a scan rate of 50mV/s*

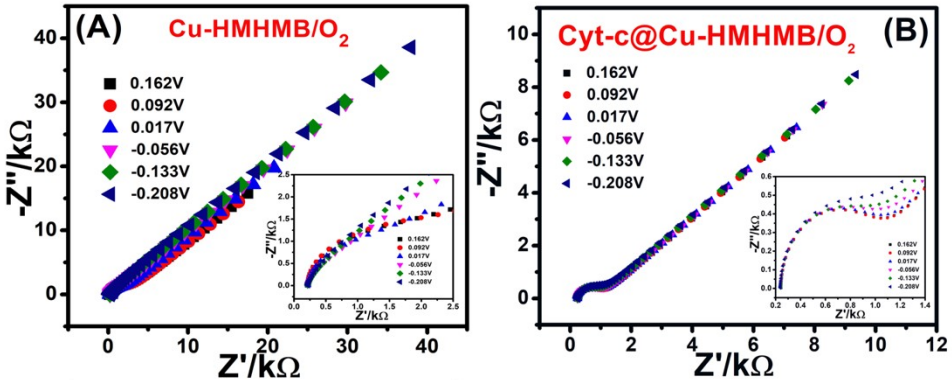

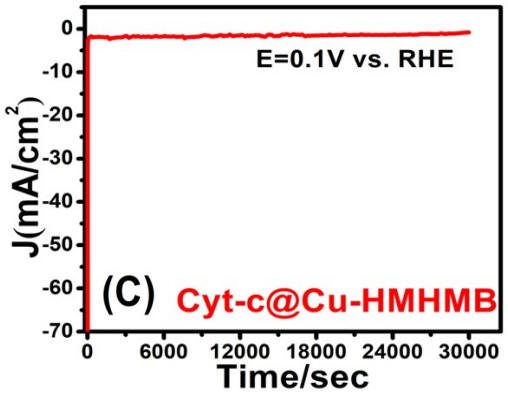

Figure-S13: *EIS studies showing Nyquist plots at varying potentials of oxygen reduction reaction over Cu-HMHMB/GCE* ***[panel-A]*** *and Cyt-c@Cu-HMHMB/GCE* ***[panel-B]****;Chronoamperometric curve at E=0.1V vs. RHE in 0.1M PBS (pH 7.2) over Cyt-c@Cu-HMHMB/GCE*

for about 30,000 seconds ***[panel-C]****.*

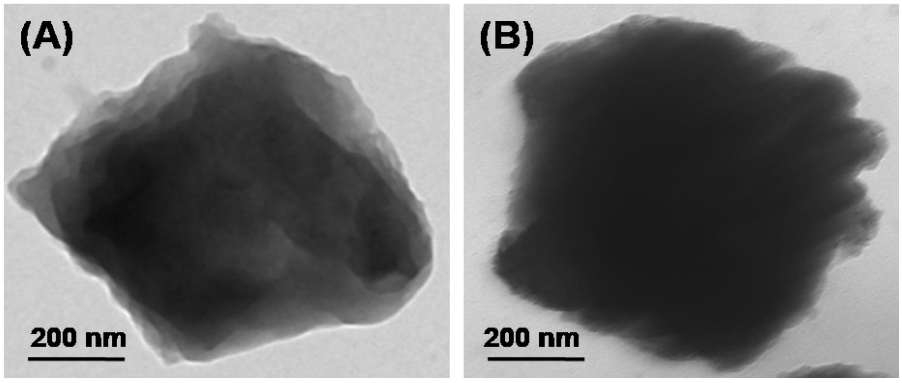

Figure-S14: *TEM image recorded for the Cyt-c@Cu-HMHMB nanocomposite pre-Electrolysis* ***[panel A]*** *and post-Electrolysis tests* ***[panel-B]***

Reference

S1. A.K. Bar, R. Chakrabarty, G. Mostafa, P.S. Mukherjee, Self-Assembly of aNanoscopic $Pt_{12}Fe_{12}$ Heterometallic Open Molecular Box Containing Six Porphyrin Walls, *Angew. Chem. Int. Ed*., 2008, **47**, 8455 –8459